SAR MONITORING OF PROGRESSIVE GROUND DEFORMATION IN ETOLIKO USING THE PERSISTENT SCATTERERS AND SBAS TECHNIQUES.

Gkartzou E., Parcharidis I. and Karymbalis E.

Harokopio University of Athens, Department of Geography, El. Venizelou 70, 17671 Athens, Greece, gkartzou@hua.gr, parchar@hua.gr, karymba@hua.gr

ABSTRACT

The Messolonghi-Etoliko lagoons complex is located in the north part of the Gulf of Patras in the central west coast of Greece. It is one of the most important Mediterranean lagoons for both environmental and financial reasons. It is a shallow area of 150 km^2, extended between the Acheloos and Evinos rivers, it is protected by the Ramsar Convention and it is also included in the Natura 2000 network. The town of Etoliko, known as the Little Venice of Greece, is a municipal section of Messolonghi municipality with a population of 5,349 inhabitants, ten kilometers northwest of Messolonghi. Etoliko is developed on a small island rooted in water in the middle of the lagoon. It is connected east and west to the mainland by two stone arched bridges with original length of about 300 meters each.

This paper studies the ground deformation of the town of Etoliko using Multitemporal SAR Interferometry techniques and more precisely, the Persistent Scatterers Interferometry Technique (PSInSAR) and Small Baseline Subset (SBAS), which have proven a remarkable potential for mapping ground deformation phenomena. This approach allows to make accurate measurements very close to its theoretical limit (in the order of 1 mm), and to obtain from the numerous radar targets very precise displacement information.

We applied the PS approach (Gamma-IPTA chain) and an ad-hoc SBAS approach on 105 SAR images from the European Remote Sensing satellites ERS-1, ERS-2 and 55 ENVISAT images that cover the two time periods, 1992-2000 and 2002-2009, to map the Etoliko subsidence.

In contrast to discrete point in-situ deformation measurement techniques, multi-temporal InSAR processing can be used to obtain a broader view of deformation processes at a site and to detect localized deformation features. Results highlight the deformation phenomena occurring the last 2 decades, showing low rate of subsidence.

Subsidence is an important hazard related with the development of urban areas. In order to have a thorough study of the ground surface deformation demands a continuous and wide spatial-temporal monitoring. By studying the deformation rates obtained by the PS technique, the lithology of the area, the sea level rise and any kind of human interventions, we can make a reliable prediction for the forthcoming years concerning the risk of flooding, the stability of the area and therefore to reduce the negative effects of these risks to humans.

Keywords: SAR interferometry, SVD, PSI, ground deformation, subsidence, Etoliko, Greece.

INTRODUCTION

In the last 20 years, InSAR and differential timeseries InSAR approaches have shown a great capability in mapping the earth surface deformation induced by various geophysical or human mechanisms. Spaceborne Synthetic Aperture Radar (SAR) interferometry has become a very useful tool for ground deformation detection and monitoring (Massonnet et al., 1993; Zebker et al., 1994).

The utilization of an appropriate interferometric dataset allows measuring various factors, such as ground deformation, subsidence, ground movement etc. Such analysis was performed in the present study to investigate the ground deformation using the PSI technique and the SBAS technique in the area of Etoliko.

The studied area is situated in the western part of central Greece (Fig. 1). The Messolonghi–Etoliko region is located about 250 km northwest from Athens, the capital of the Greek Republic and is bordered in the north-west of the Messolonghi lagoon at a distance of 10 km Southeast of Messolonghi. It is part of the Natura 2000 (GR2310002) and protected wetland under the Ramsar Convention. The latitude and longitude of the study area are 38◦26 and 21◦21 respectively. Morphologically, the study area can be characterized as flat area with an altitude of 6 meters. The lagoon of Messolonghi bordered to the south of the Gulf of Patras, communicates through openings formed between a series of sandy islands with a total length of about 12Km. It is a shallow lagoon with an average depth of about 0,5m and a maximum of 3m.

In the northern part of the lagoon extends Etoliko, which for the most part, has a depth of about 5-10m, except for the northern part where the depth reaches 33m. The two lagoons communicate through two bridges with an average depth of approximately 80cm and a length of 80m each (Kountoura & Zacharias, 2009). The Messolonghi-Etoliko lagoon complex is a huge biotope and part of the most important and valuable ecosystem defined by the mouth of Evinos river to the mouth of Acheloos river (Fig.1). Source of wealth and prosperity the lagoon for both cities but especially for the city of Etoliko, which was born several hundred years before Messolonghi, literally in the heart of the lagoon and has an integral role on this great ecosystem, the largest in Europe (Http://en.wikipedia.org/wiki/Etoliko).

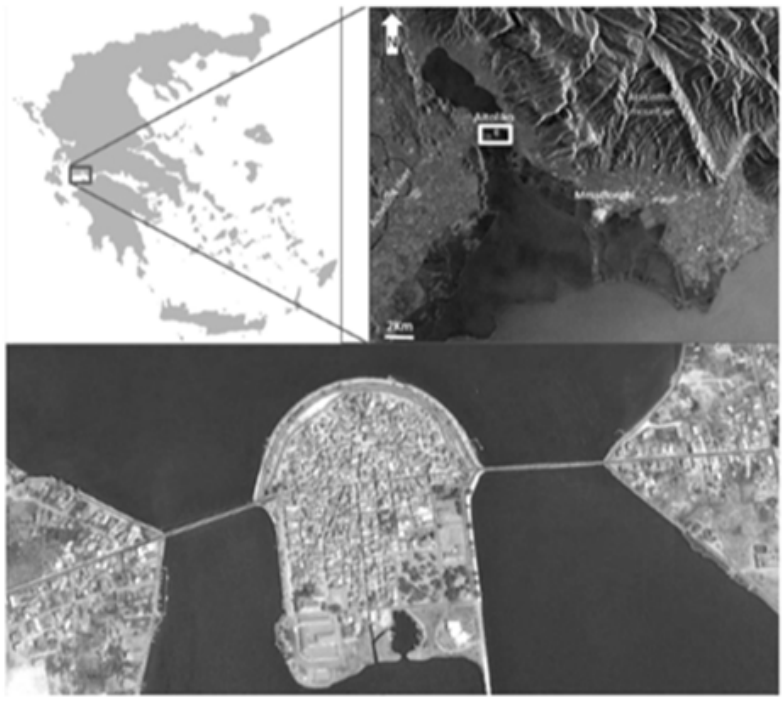

Figure 1: Study area

Geology – seismicity

Etoliko is situated in Aetolia, West Greece, together with Acarnania, Aetolia forms one of the largest western prefecture of Central Greece, Aetolacarnania. Aetolia is characterized by a rugged mountainous interior. Covering almost the entire district, the southern Pindos Mountains belong to the Hellenides, a southern branch of the Alpidic orogenic belt (Kokinou et al., 2005).

The study area lies within the Ionian Zone of the West Hellenic Nappe of the External Hellenides (Vött, 2007). During the Miocene, tectonic activity shifted to the Hellenic arc which extends from Ionian Islands in the west, passing Crete in the south to the island of Rhodes in the east (Brooks et al., 1988;Kokinou et al., 2005).

Aetolias mountainous hinterland is opposed to the shallow coastal plain shaping its southwestern most border. Ongoing delta progradation by the Acheloos and Evinos, both originating in the southern Pindos Mountains, resulted in silting up of the shelf region of the Gulf of Patras forming a large, overlapping delta (Piper and Panagos, 1981). While the Evinos delta still drains into the Gulf of Patras, the Acheloos River delta can be subdivided into a recent, western delta discharging into the Ionian Sea and a subrecent, eastern delta which merged with the Evinos delta to form a large coastal plain (Piper and Panagos, 1981). The petrography of the overlapping delta reflects the bedrock. The sand fraction of both deltas is predominantly composed of carbonate, chert and quartz whereas feldspar, heavy minerals and mica play a secondary role. The fine fraction is dominated by montmorillonite, illite and poorly crystallized chlorite while calcite quartz and feldspar are a minor constituent (Kontopoulos and Panagos, 1980). On the delta plain, an extensive lagoon complex developed of which the Etoliko Lagoon marks the northern part.

To the north and east, the lagoon is flanked by the Arakynthos Mountains composed of Palaeogene limestones partly overlain by sand and siltstones (Flysch). The western part of the lagoon is bordered by Triassic limestone and gypsum breccias of the Aghios Ilias ridge and Pliocene conglomerates and marls of the Aghios Nikolaos mound. Those two elevations are intersected by a low land pass referred to as the Paracheloïtis low land pass (PLP) with a width of only 1 km. To the south, the Etoliko basin communicates with the shallow Messolonghi lagoon which is separated from the Gulf of Patras by sandbars forming long and narrow islets (Vött et al., 2007).

By studying the seismicity of the area from the beginning of the last century, the only earthquake that affected Etoliko with serious damages was in March 1965 in Agrinio with a magnitude of 6.8R which destroyed buildings and infrastructures and caused the collapse of the church. The rest of the earthquakes occurred close to Messolonghi, have a magnitude below 4R. Also, as we can see in the seismic hazard map of Greece, the area of Messolonghi-Etoliko belongs to a low level hazardous area.

The lagoon settings

The Etoliko Lagoon covers an area of 17 km^2. The strong tectonic influence on its formation explains the great depth of around 30m at its profundal zone. In its southern part where the Etoliko basin is connected with the Messolonghi Lagoon it is characterized by shallow waters with a maximum depth of <1m (Vött et al., 2007).

The limited connection with the Messolonghi Lagoon, insufficient freshwater inflow, and the morphology of the lagoon itself lead to a permanently stratified water column caused by a well-developed salinity gradient (Papadas et al., 2009). Hence, key physical characteristic of the lagoon are permanent thermocline and halocline and an anoxic hypolimnion which favors the preservation of finely laminated sediments in central-distal areas of the lagoon. The main feature of the Etoliko lagoon is the anoxic conditions that characterize the deeper layers, as well as the high concentrations of H_2S occurring in them, as a result of both the geology of the region

(the presence of gypsum) and the decomposition of organic materials (Leonardos and Sinis, 1997).

The lagoon is characterized by strong-permanent stratification in salinity which prevents the vertical mixing of water and maintaining subacetate-anoxic conditions in deeper waters. The salinity of surface and coastal waters is low, to the levels of slightly brackish values. The low salinity is due to the inflow of irrigation water and the limited contact of the area with the Messolonghi lagoon and through it with the open sea. The recent hydrological network is strongly influenced by anthropogenic activities. Several natural streams draining the Lagoon from the adjacent mountains have been canalized and are now acting as irrigation and/or drainage systems. They enter the lagoon via four pumping stations (Gianni et al., 2011).

Climate

Characterized by a high seasonality with hot, dry summers and mild, wet winters, recent climate in the study area reflects the outlined large scale circulations patterns. The average annual temperature ranges from 17 to 18 ºC with an annual thermometric width range from 18 to 19 ºC.

The region experiences high spatial and temporal variability of rainfall additionally controlled by sharp hydrological gradients resulting from high relief differences with approximation to the mountainous interior. Hence, rivers and creeks originating in the mountains strongly reflect humid mountain climate which may trigger distinct flood events and the reactivation of ancient river channels (Weischet and Endlicher, 2000). The coldest month is January with an average air temperature of 9 ºC whereas in July and August the average air temperature is 27 ºC but may reach 40 ºC. This results in a negative water balance with loss of up to 1540 mm/a due to evaporation which strongly affects water level and physicochemical characteristics of the lagoon (Gianni et al., 2011).

The average annual rainfall is around 800-1000 mm with most rainy period from November to February. The rainfall occurs during the months October to April, resulting in a 4.5-month dry season (May-September). The average annual relative humidity ranges from 64-68% in both coastal zone (meteorological station Technological Institute of Messolonghi), and within the county, mainly because of large bodies of water.

During the summer months (dry season) prevailing westerly winds, while all the other months mostly south - southwestern and north - northwestern. Rarely appear in the area eastern winds, mainly because of the mountain range of Pindos, which forms a natural boundary to the east of the prefecture (YP.E.CH.O.D.E. / Directorate of Water and Natural Resources).

DATA USED AND METHODOLOGY

For the scope of the study, a total number of 33 ERS-1&2 and 21 ENVISAT ASAR scenes were acquired along the ascending track 186 and 43 ERS-1 & 2 -and 27 ENVISAT ASAR scenes were acquired along the descending track 50, covering the period between 1994 and 2001 (~7 yr) and 2002-2010(~8 yr) respectively and were processed using the GAMMA™ software. All data were obtained from the European Space Agency (ESA). The selection and order of the images were made using the EOLi software (http://earth.esa.int/EOLi.html) and they cover the surrounding area (Fig.2). Initial estimations of the interferometric baselines were calculated from the Deflt precise orbit state vectors (Scharoo and Visser, 1998). The topographic phase was simulated based on SRTM V3 DEM of approximate spatial resolution of 90 m.

The main processing steps followed for the whole data set comprise the conversion of raw data to SLC while updating their parametric files with the orbit data, co-registration and cropping of SLCs, simulation of the topographic phase, generation of differential interferograms, filtering and phase unwrapping.

Figure 2: Dataset selection through EOLi software, ESA. The dataset selection is shown with the yellow box.

The data obtained after all these procedures were processed using two different interferometric techniques, the Persistent Scatterers Interferometry Technique (PSInSAR) and the Small Baseline Subset (SBAS)/SVD method, which have proven a remarkable potential for mapping ground deformation phenomena with accurate measurements very close to 1 mm (Elias et al., 2009).

Subsidence estimation around Etoliko using the Persistent Scatterers Interferometry Technique

The PS technique is a fully operational powerful tool allowing to exploit long series of interferometric SAR data aiming at high-precision ground deformation mapping. Moreover, since PS are point-wise targets whose elevation is known with high precision as well, deformation data can be mapped on the corresponding structures. This advanced multi-temporal approach called the Permanent Scatterers (PS) technique was introduced by Ferretti et al in 2000, the first team who defined this technique to measure and monitor ground deformation by millimetric precision. The differential interferometric methodology that will be used in this study was basically the PSI based on the Interferometric Point Target Analysis (IPTA) algorithm included in GAMMA software.

It is a two-step technique which firstly allows the identification and then the use of natural stable scatterers which are only slightly disturbed by decorrelation noise such as buildings, rocks, etc. starting from a multi-temporal database of interferometric images. The first identification phase make possible to extract these pixels based on selected criteria. Then, the ground movement estimation is done starting from these reliable and precise pixels phase values and generalized on the entire image. The PS approach allows the isolation of different phase terms on a sparse grid of phase stable radar targets and it is based on the exploitation of time-series of interferometric data.

From these two-steps we produce two candidate point lists, we merge them into a single one which is therefore been used for the analysis. A total number of 130896 and 58318 candidate points for ERS ascending and ERS descending dataset respectively, were determined. The spatial distribution of the candidate points is not homogeneous with high densities of PS located in built-up and mountainous areas and low densities over fields. The IPTA methodology requires one single scene as reference in order to form multiple pairs and produce interferograms. In order to select the best suitable reference scene we have to check that the acquisition date is in the middle of the time frame for which there are available SAR acquisitions and also the produced interferometric pairs to have the minimum perpendicular baseline (Bp). Also the reference scene must present low atmospheric distortions. For the ERS ascending dataset the best suitable scene was August 25, 1996, with an average Bp of 400 m and for the ERS descending dataset was December 19, 1997, with an average Bp of 373m.

Afterwards the initial differential interferograms were produced by simulation of the unwrapped interferometric phase based on the initial baselines and the DEM. Thus, processing proceeds by applying a least-squares regression on the differential phases in order to estimate terrain height and deformation rate relative to a reference point target. The reference point is selected in a considered stable area and it is the point from which the unwrapping of the differential interferograms will begin.

Based on the regression analysis, the quality of the PS candidates was further evaluated through the estimated standard deviation of the phase difference and many PSs with a phase standard deviation larger than the indicated were rejected, significantly reducing the number of points. The majority of the rejected points were located over mountainous areas. The PSs were further processed in order to compensate atmospheric and noise effects. Thus, residual phases were spatially filtered by applying a low-pass spatial filter. The generated results consist of height corrections, linear deformation rates, atmospheric phase, refined baselines, temporal coherence, and nonlinear deformation histories for each scatterer. Finally the deformation phases were transformed into displacements and geocoded to the selected cartographic reference system (UTM, WGS84).

Subsidence estimation of Etoliko using Singular Value Decomposition (SVD) method

For our purpose, we have applied the DInSAR technique, which is based on exploiting the phase difference (interferogram) between SAR image pairs acquired at different times; this allowed to extract information along the radar line of sight (LOS) projection of the displacements that occurred between acquisitions (Gabriel et al., 1989; Massonnet et al., 1993). In particular the algorithm used is the one referred to as Small Baseline Subset (SBAS) approach (Berardino et al., 2002) that relies on an appropriate combination of the DInSAR interferograms by using subsequently acquired SAR data. Moreover, to reveal the deformation history, Singular Value Decomposition (SVD) method was implemented (Berardino et al., 2002; Usai, 2003). The SVD method allowed to easily “link” independent SAR acquisition data set separated by large spatial baselines, thus increasing the number of data used for the analysis of the area of interest (Manzo et al., 2005). The data used to generate the interferograms are characterized by a small spatial and temporal separation between the orbits, in order to limit the noise effects usually referred to as decorrelation phenomena (Zebker and Villasenor, 1992).

For the period 1995-2001 (ERS-1&2) perpendicular baselines up to 200m and time interval up to 2 years in both ascending and descending orbit were accepted in order to form a sufficient network. On the other hand, from the period 2003 to 2010 (ENVISAT) perpendicular baselines up to 400m and time interval up to 3 years in ascending orbit and Bp up to 350m along with 2 years of temporal separation in descending orbit for each acquisition to form interferograms, were selected. Based on above parameters, networks were established, which reflected the date of receipt of each image, relative to the baseline, as well as the pairs of images which produced conventional interferograms.

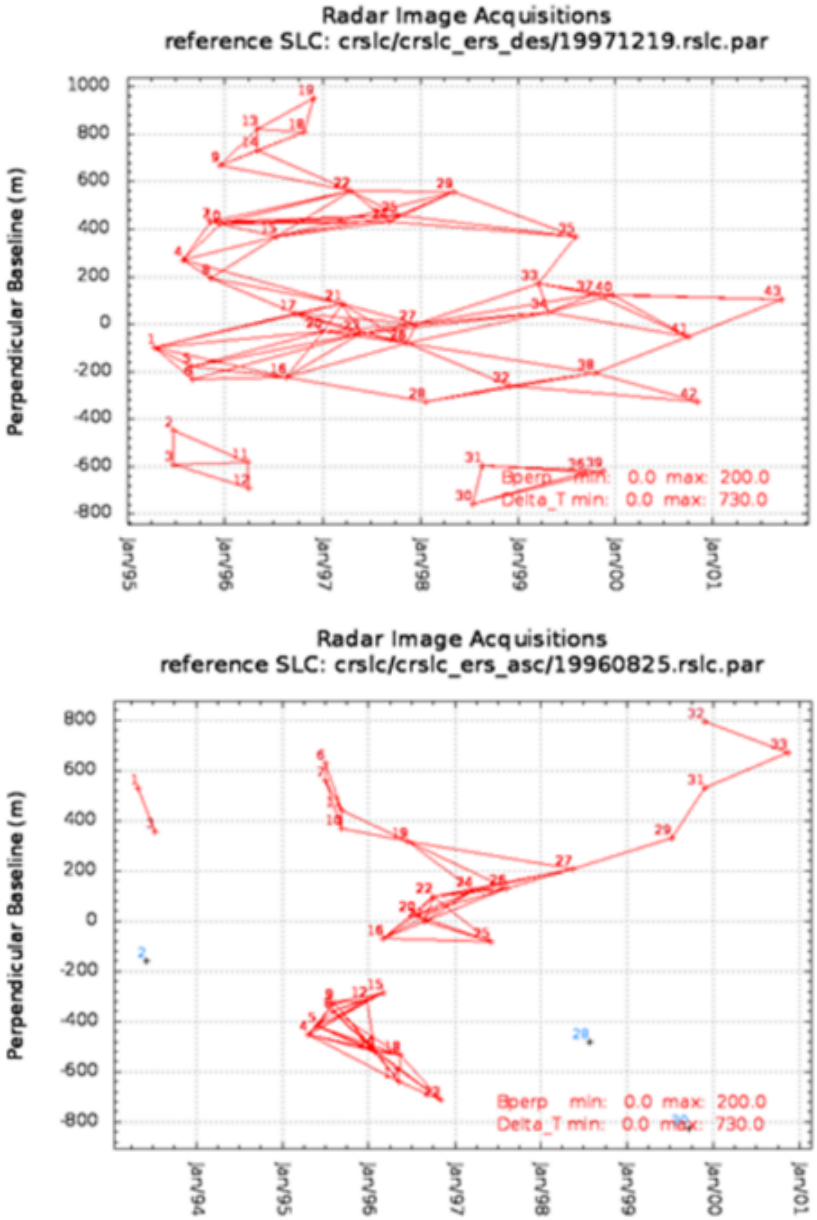

Figure 3: Network of ERS-1&2 ascending (on the top) and descending (below) for the period 1994-2001

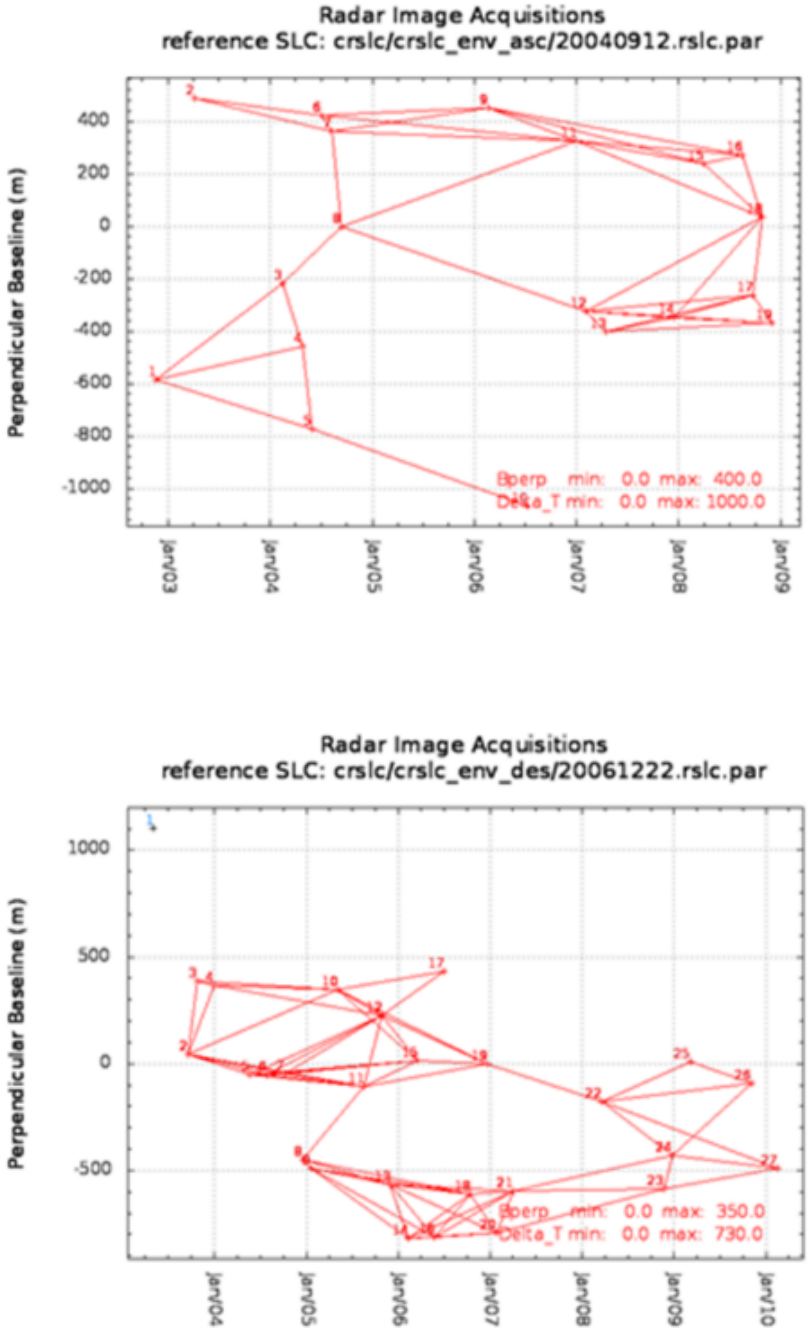

Figure 4: Network of Envisat ascending (on the top) and descending (below) for the period 2003-2010

Figures 3 and 4 depict the produced networks. The interferograms produced were further analyzed and filtered using adaptive filtering. This approach tries to increase the temporal sampling rate and to provide spatially dense deformation maps by using small baseline interferograms.

The next step is related with unwrapping the adaptive interferograms using the minimum cost-flow algorithm. The threshold for the average coherence across all interferograms was set to 0.35. The reference point was carefully selected on stable ground 9 Km western of Etoliko, in Katochi village (fig.7). This procedure was repeated using precision baselines in order to decide which interferograms are going to be selected as input to the SVD solution.

After selecting the reference point, it is applied the SVD algorithm which allows the passing from the single reference acquisitions to multiple reference ones. The produced result was a product in a raster format with the accumulated phases, which reflects the average rate of phase change per time (rad/year) and also a pixel based time series analysis. In order to visualize the values of the deformation patterns derived from the SVD solution they were geocoded back from the Range Doppler Coordinates to Universal Transverse Mercator (UTM) coordinates and plotted to the DEM of the region.

RESULTS AND DISCUSSION

After processing our datasets with the two Differential Interferometric techniques, we are ready to present the final results. By transforming the interferometric results from range–Doppler coordinates into map geometry, the interferometric analysis results were imported in a GIS environment for further interpretation. The final cartographic products were obtained by using the Arc Map GIS software, which was also used for the visualization of the generated results as a geographical basis in order to display the observation and identification of the results.

At this point it should also be mentioned that regarding the stability of the reference points, it is assumed that they were selected in a stable area, but there is a possibility that the points are not absolutely stable. Therefore the resulting deformation rates are relative measurements to the 'stable' reference point, so when the terms of subsidence or uplift is used, it is always relative to the reference point.

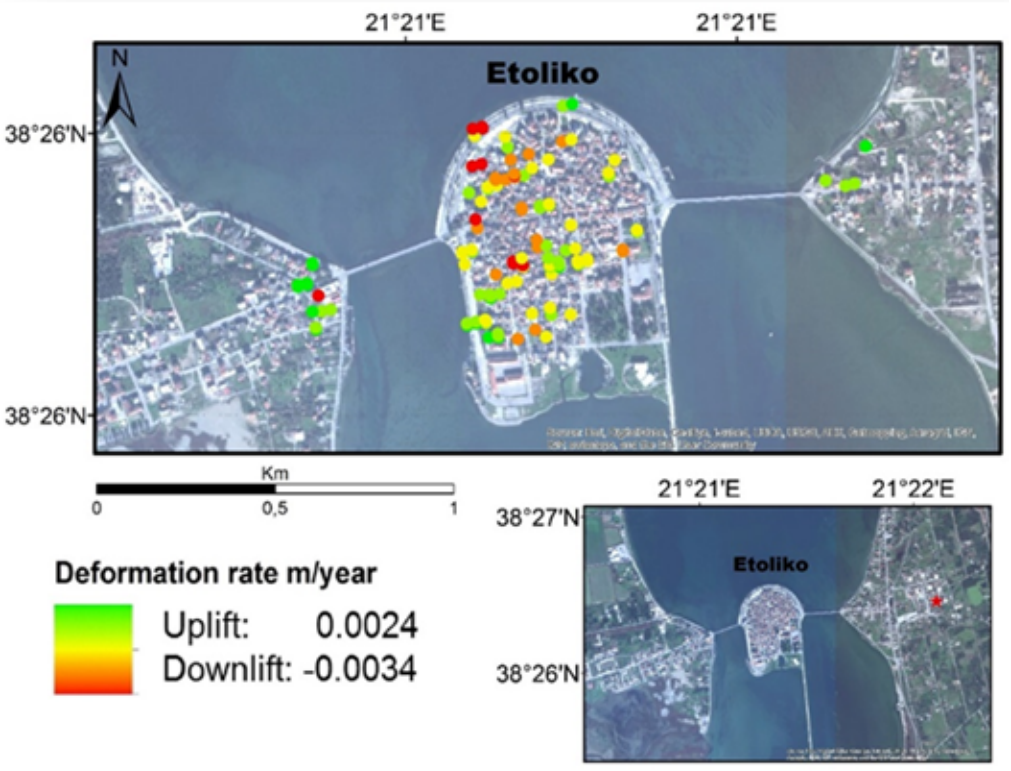

Figure 5: PSI map of the surface deformation rate of Etoliko, for the period 1994-2001, in the LOS direction (satellites ERS-1&2, ascending track). The red star in the small map represents the reference point.

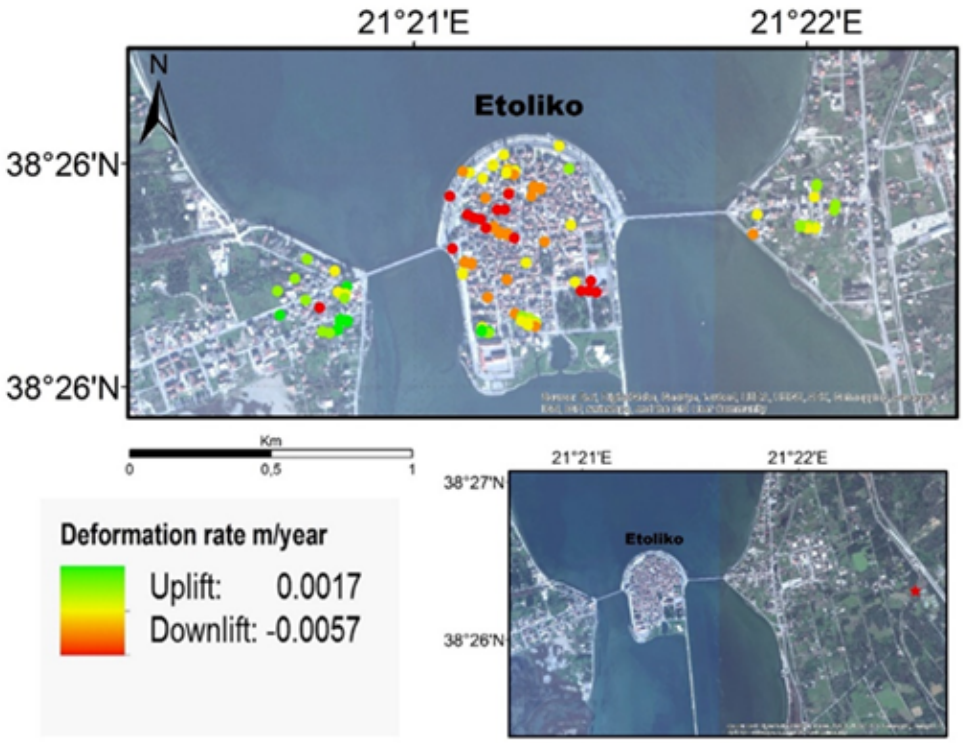

Figure 6: PSI map of the surface deformation rate of Etoliko, for the period 1994-2001, in the LOS direction (satellites ERS-1&2, descending track). The red star in the small map represents the reference point.

After processing the data of SAR satellite systems, ERS-1&2 and ENVISAT, the final maps of surface deformation, over time, were produced for both PSI and SVD techniques, as well as time-series analysis for selected points in the area of Etoliko. PSI method was applied first, in order to have a primary evaluation of the deformation in the area of interest. In figure 5 and 6, Etoliko comparing to the reference point, presents a maximum subsidence of -3,4mm/year and a maximum uplift of 2,4mm/year, but in general we can observe that the area of Etoliko shows a temporal stability with a tension to subsidence as expected due to the geology of the area characterized by the presence of alluvium, and also by the fact that the whole area is surrounded and therefore affected by water.

After having processed the PSI technique, the SVD method was applied in order to obtain a better view of the deformation rate of the area. The SVD maps of the surface deformation rate (fig.7-10) seem to follow the same pattern as the PSI maps showing stability with a tension to subsidence. More specifically, for the period 1994-2001 we observe a maximum subsidence rate of 5,5mm/year from the satellite data of ERS-1&2 and 9,4mm/year maximum subsidence from the satellite data of ENVISAT for the period 2003-2010.

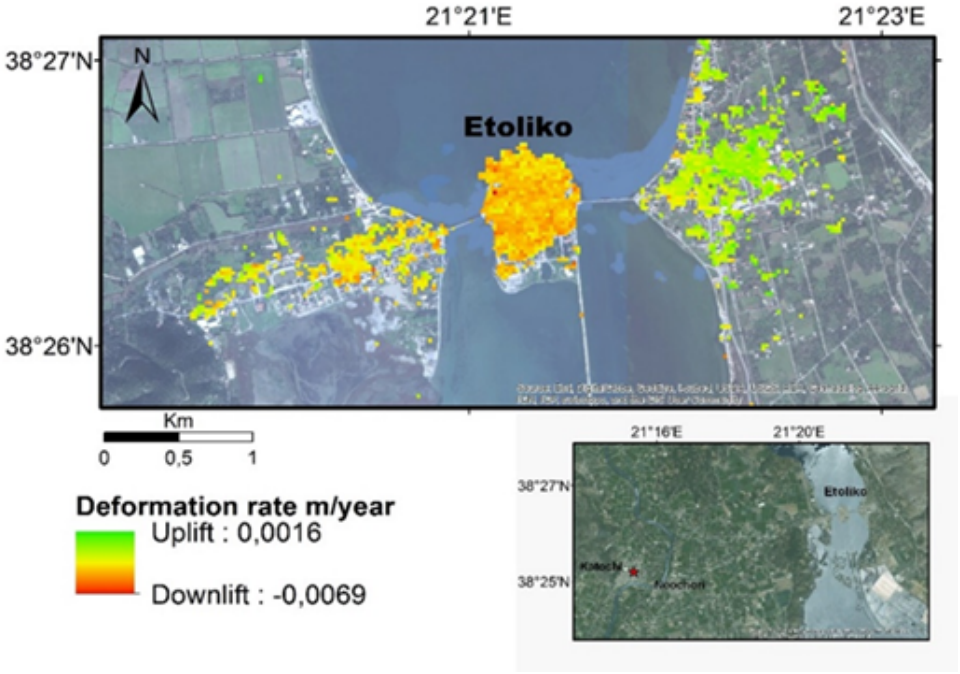

Figure 7: SVD map of the surface deformation rate of Etoliko, for the period 2003-2010, in the LOS direction (satellite ENVISAT, ascending track). The red star in the small map represents the reference point.

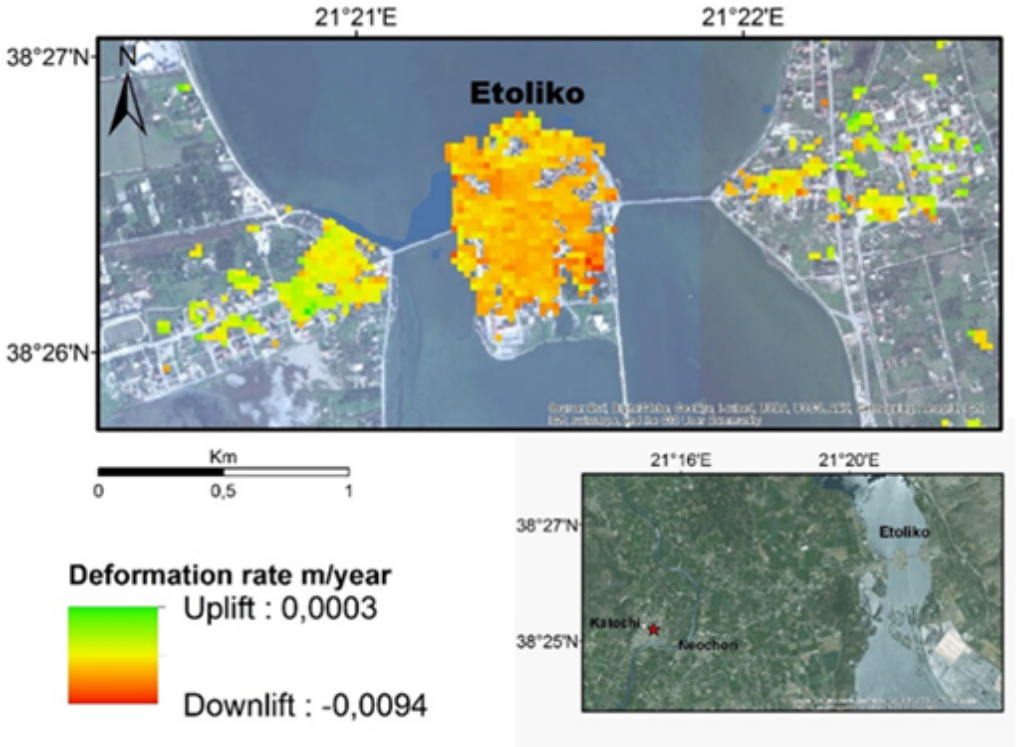

Figure 8: SVD map of the surface deformation rate of Etoliko, for the period 2003-2010, in the LOS direction (satellite ENVISAT, Descending track). The red star in the small map represents the reference point.

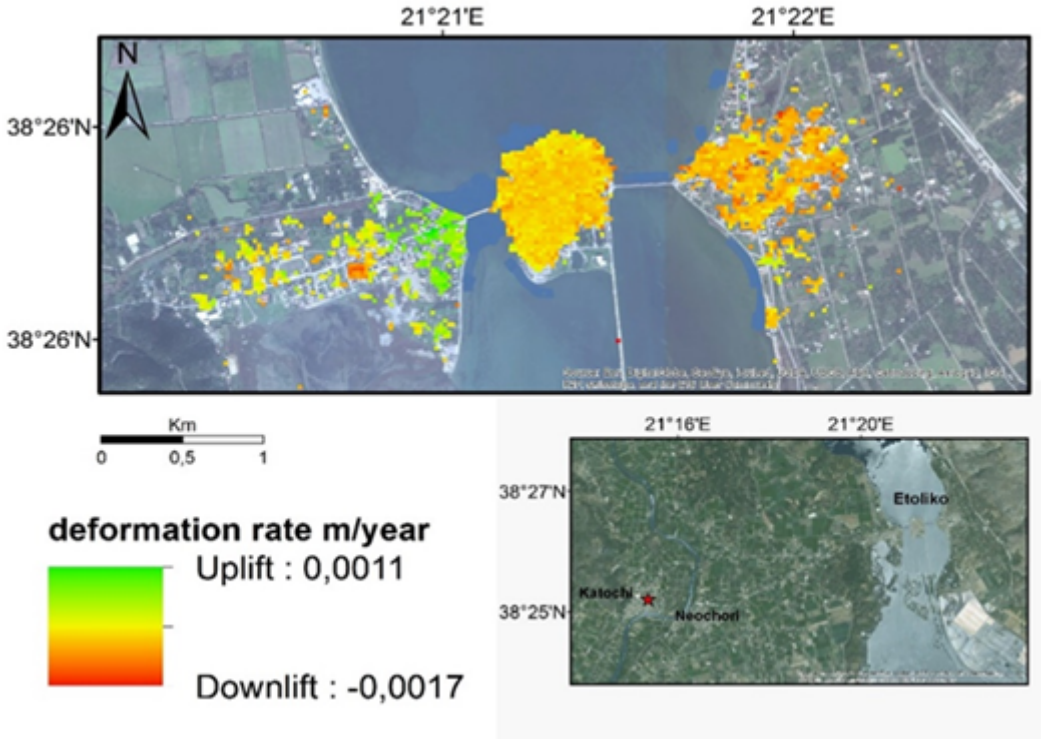

Figure 9: SVD map of the surface deformation rate of Etoliko, for the period 1994-2001 in the LOS direction (satellites ERS1&2, ascending track). The red star in the small map represents the reference point.

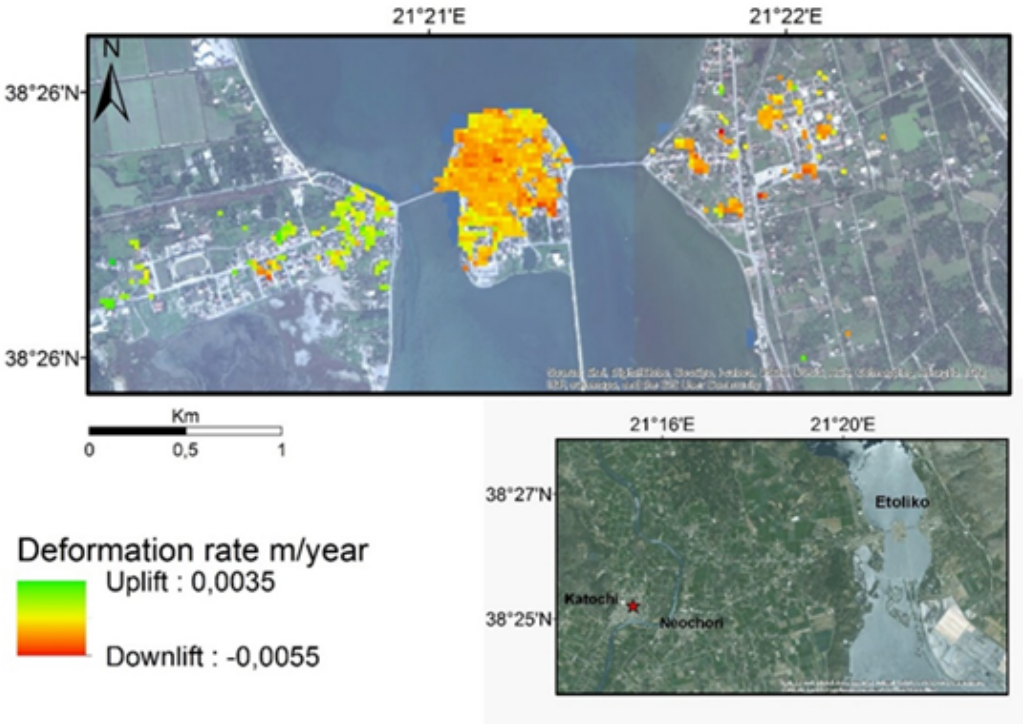

Figure 10: SVD map of the surface deformation rate of Etoliko, for the period 1994-2001 in the LOS direction (satellites ERS1&2, descending track). The red star in the small map represents the reference point.

Figure 11: Selected points P1 & P2 where time-series analysis was applied

In order to apprehend better the results, it was considered appropriate to create diagrams of the temporal deformation by selecting two randomly selected points, one in the center of the area P1 and the other aside to the area in the northern part P2 (Fig.11).

From the charts it can be observed that points P1 and P2 present exactly the same pattern of temporal deformation and by analyzing them, it is noticeable that the specific two points are pretty much stable with maximum uplifts and downlifts between 10 and-10mm/year.

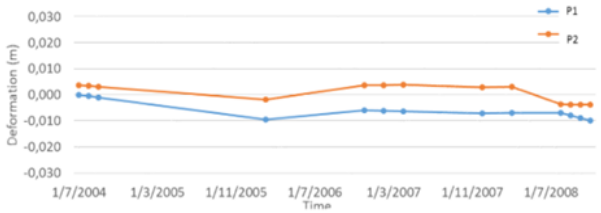

Figure 12: Temporal Deformation Chart for selected points P1 & P2 (Satellite Envisat, Ascending track)

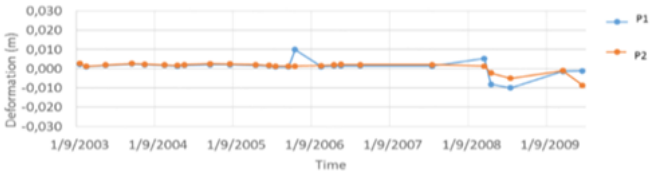

Figure 13: Temporal Deformation Chart for selected points P1 & P2 (Satellite Envisat, Descending track)

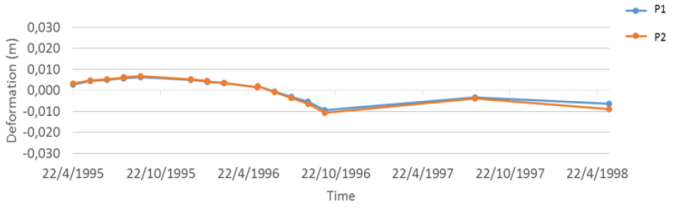

Figure 14: Temporal Deformation Chart for selected points P1 & P2 (Satellites ERS-1&2, Ascending track)

Figure 15: Temporal Deformation Chart for selected points P1 & P2 (Satellites ERS-1&2, Descending track)

Multitemporal SAR Interferometry techniques were applied to study the temporal evolution of ground deformation in Etoliko. By the analysis it was allowed to describe the deforming behavior of Etoliko through PSI and SVD approaches, respectively. The results retrieved subsidence specifically close to the two bridges of Etoliko, in the eastern and western part.

From the PSI map of the surface deformation rate of Etoliko for the period 1994-2001, it can be seen that the average deformation rates are mostly between 2 and -4mm/year, while at the same time the SVD results for the same period showing average rates of the same levels. Additionally it is interesting to note that for both applied techniques the highest subsidence is observed at the same parts of Etoliko.

CONCLUSIONS

The major advantages of the PS approach are a remarkable precision coupled with a high spatial density of benchmarks. A further interesting property is the availability of point displacement data, enabling to describe motion affecting individual structures. On the other hand, the main limit is related to the intrinsic ambiguity of phase measurements that prevents the technique from being able to monitor rapidly evolving deformation phenomena (Colesanti et al., 2003).

Moreover, a sufficient spatial PS density (5–10 PS/km) is required to properly estimate and remove atmospheric artifacts, and at least about 25 images are necessary to fulfill a reliable PS analysis.

Persistent Scatterers Interferometry (PSI) served as a methodology of ground deformation detection and estimation for the broader area of the Messolonghi-Etoliko, for the time period between 1994 and 2001, as well as the SVD technique which in addition shows results also for the time period 2003-2010. In the study area the main cause of ground subsidence seems to be the natural compaction of the loose sediments as it is well known that Etoliko was primarily a cluster of four or five very small islands close to each other, in the center of the lagoon which were covered by the water during the winter. The first inhabitants, which were mostly fishermen, joined them initially with small wooden bridges and with continuous embankments shaped the small island. The last embankment was in 1972 over a large area north and south of the small island which changed completely the form of the island in order to gain plots for buildings. The reason for this historic reference is mainly to verify the results of the processing and to identify the cause of the subsidence.

The PS technique is a fully operational powerful tool allowing to exploit long series of interferometric SAR data aiming at high-precision ground deformation mapping. The precision of the technique achieves values of 1–3 mm on individual measurements and 0.1–0.5 mm/year on the average deformation rate. Moreover, since PS are point wise-targets, whose elevation is known with high precision as well, deformation data can be mapped on the corresponding structures (Ferretti et al, 2001).

The precision assessment of the technique deserves further studies, in particular to investigate the spatial lowpass error increasing with the distance from the ground control point PS results are relative to. A further research issue is the combination of PS data relative to adjacent tracks and ascending and descending passes in order to increase the PS spatial density and to cross-validate results (Colesanti et al., 2002), as well as to map deformation along two independent dimensions.

ACKNOWLEDGMENTS

We would like to thank the European Space Agency (ESA) for their support via their projects and the data supply for this research.

REFERENCES

Becker, R.H. and Sultan, M., 2009. Land subsidence in the Nile Delta: inferences from radar interferometry. The Holocene, 19, 949–954.

Berardino P., Fornaro G., Lanari R. and Sansosti E., 2002. A new algorithm for surface deformation monitoring based on the combination of small baseline DInSAR interferograms, IEEE Trans.Geosci.Remote Sens., vol. 40, pp. 2375–2383.

Brooks, M., Clews, J., Melis, N., Underhill, R., 1988. Structural development of Neogene basins in western Greece. Basin Research 1, 129-138.

Colesanti C., Ferretti A., Prati C., and Rocca F., 2002. Full exploitation of the ERS archive: Multi data set permanent scatterers analysis, Proc. IGARSS.

Dassenakis, M., Krasakopoulou, E., Matzara, B., 1994. Chemical characteristics of Aetoliko lagoon, Greece, after an ecological shock. Marine Pollution Bulletin 28, 427-433.

Elias P., et al., 2009. Permanent Scatterer InSAR Analysis and Validation in the Gulf of Corinth. Sensors 2009, 9, 46-55; doi:10.3390/s90100046.

Ferretti A, Prati C, Rocca F., 2000. Nonlinear subsidence rate estimation using permanent scatterers in differential SAR interferometry. IEEE Transactions on Geoscience and Remote Sensing 38(5):2202-2212.

Ferretti A., Prati C., and Rocca F., 2001. Permanent scatterers in SAR interferometry, IEEE Trans. Geosci. Remote Sensing, vol. 39, pp. 8–20.

Gabriel A. K. , Goldstein R. M. , and Zebker H. A., 1989. Mapping small elevation changes over large areas: Differential radar interferometry, J. Geophys. Res., vol. 94.

Gianni, A., Kehayias, G., Zacharias, I., 2011. Geomorphology modification and its impact to anoxic lagoons. Ecological Engineering 37 (11), 1869-1877.

Gianni, A. and Zacharias, I. 2011. Anoxia, hydrogen sulfide and storm events in Etoliko lagoon, Greece. Proceedings of the 3rd International CEMEPE & SECOTOX Conference, Skiathos, June 19-24, 2011, ISBN 978-960-6865-43-5, 125- 130.

Haenssler, E., et al., 2013. Natural and human induced environmental changes preserved in a Holocene sediment sequence from the Etoliko Lagoon, Greece: New evidence from geochemical proxies. Quaternary International, 308-309, 89-104, doi:10.1016/j.quaint.2012.06.031

Karapiperis,L., 1974.Rainfall distribution in Greece. Bulletin of the Geological Society of Greece, 11, 1–27.

Kokinou, E., Kamberis, E., Vafidis, A., Monopolis, D., Ananiadis, G., Zelilidis, A., 2005. Deep seismic reflection data from offshore western Greece: a new crustal model for the Ionian Sea. Journal of Petroleum Geology 28 (2), 185-202.

Kontopoulos, N., Panagos, A., 1980. Morphological analysis of pebbles from the Evinos River. Bulletin of the Geological Society of Greece.

Kountoura, K., Zacharias, I, 2009. Study of the refreshment rate of water in the Etoliko lagoon, 9th Greek Symposium of Oceanography & Fisheries, Proceedings, Volume II, 1235-1240. (in Greek with English abstract).

Leonardos, I., Sinis, A. 1997. Fish mass mortality in the Etolikon lagoon, Greece: The role of local geology. Cybium 21, 201-206.

Massonnet, D.; Rossi, M.; Carmona, C.; Adragna, F.; Peltzer, G.; Feigl, K., and Rabaute T., 1993. The displacement field of the Landers Earthquake mapped by radar interferometry. Nature, 364, 138–142.

Papadas, I.T., Katerinopoulos, L., Gianni, A., Zacharias, I., Deligiannakis, Y., 2009. A theoretical and experimental physicochemical study of sulfur species in the anoxic lagoon of Aitoliko-Greece. Chemosphere 74, 1011-1017.

Piper, D.J.W., Panagos, A.G., 1981. Growth patterns of the Acheloos and Evinos deltas, western Greece. Sedimentary Geology 28 (2), 111-132.

Usai S. 2003. A least squares database approach for SAR interferometric data, IEEETrans. Geosci. RemoteSens, vol.41,no.4 , pp.753–760.

Vött, A., Schriewer, A., Handel, M., Brückner, H., 2007. Holocene palaeogeographies of the Eastern Acheloos River Delta and the Lagoon of Etoliko (NW Greece). Journal of Coastal Research 23, 1042e1065.

Vött, A., 2007. Relative sea level changes and regional tectonic evolution of seven coastal areas in NW Greece since the mid-Holocene. Quaternary Science Reviews 26, 894-919.

Weischet, W. & Endlicher, W., 2000. Regional Climatology, Part 2: The old world, Stuttgart. (in Greek with German abstract).

Zebker H. A. and Villasenor J., 1992. Decorrelation in interferometric radar echoes, IEEE Trans. Geosci. Remote Sensing, vol. 30, pp. 950–959.

Zebker, H.A.; Rosen, P.A.; Goldstein, R.M.; Gabriel, A., and Werner, C.L., 1994. On the derivation of coseismic displacement-fields using differential radar interferometry—the Landers earthquake. Journal of Geophysical Research–Solid Earth B, 10, 19617–19634.